Published in final edited form as:
*Nano Lett*. 2009 October ; 9(10): 3482–3488. doi:10.1021/nl901681d.

# Suppressed Auger Recombination in "Giant" Nanocrystals Boosts Optical Gain Performance

**Florencio García-Santamaría**, **Yongfen Chen**, **Javier Vela**, **Richard D. Schaller**, **Jennifer A. Hollingsworth**, and **Victor I. Klimov***
Chemistry Division and Center for Integrated Nanotechnologies, Los Alamos National Laboratory, Los Alamos, New Mexico 87545

## Abstract

Many potential applications of semiconductor nanocrystals are hindered by nonradiative Auger recombination wherein the electron–hole (exciton) recombination energy is transferred to a third charge carrier. This process severely limits the lifetime and bandwidth of optical gain, leads to large nonradiative losses in light-emitting diodes and photovoltaic cells, and is believed to be responsible for intermittency ("blinking") of emission from single nanocrystals. The development of nanostructures in which Auger recombination is suppressed has recently been the subject of much research in the colloidal nanocrystal field. Here, we provide direct experimental evidence that so-called "giant" nanocrystals consisting of a small CdSe core and a thick CdS shell exhibit a significant (orders of magnitude) suppression of Auger decay rates. As a consequence, even multiexcitons of a very high order exhibit significant emission efficiencies, which allows us to demonstrate optical amplification with an extraordinarily large bandwidth (>500 meV) and record low excitation thresholds. This demonstration represents an important milestone toward practical lasing technologies utilizing solution-processable colloidal nanoparticles.

Colloidal semiconductor nanocrystals (NCs) have been the subject of intense research due to potential applications in low-threshold lasers, biological tags, third-generation photovoltaics, and light-emitting diodes (LEDs).[1,2] All of these technologies can benefit from the unique properties of NCs such as a size-tunable energy gap, high photoluminescence (PL) quantum yields, good stability, and chemical processability. However, many of these potential applications are hindered by Auger recombination, wherein the energy of one electron–hole pair (exciton) is nonradiatively transferred to another charge carrier.[3] In NCs, this process occurs on subnanosecond time scales and reduces optical gain lifetime,[4] restricts the available time to extract multiple excitons generated via carrier multiplication,[5] limits LED brightness due to the build-up of charged NCs,[6] and leads to PL intermittency ("blinking") that is typically observed in single-NC studies.[7,8]

While the physics underlying Auger recombination in NCs is still not fully understood, general considerations suggest that the rate of this process is directly dependent upon the strength of carrier–carrier Coulomb coupling and the degree of spatial overlap between the electron and hole wave functions involved in the Auger transition.[9–11] Previous approaches to reducing Auger recombination rates have utilized the manipulation of both of these parameters. For example, using elongated NCs (quantum rods), one can separate interacting excitons along the rod axis, which leads to decreased exciton–exciton Coulomb coupling.[12] Also, one can reduce the rate of Auger transitions by separating electrons and holes between the core and the shell

*To whom correspondence should be addressed. klimov@lanl.gov.

Supporting Information Available: This material is available free of charge via the Internet at http://pubs.acs.org.

regions of core–shell heterostructured NCs that exhibit so-called type-II or quasi-type-II localization regimes.[13,14] The latter approach has been especially successful in the case of CdTe(core)/CdSe(shell) nanostructures, as indicated by a recent observation of intense multiexciton lines in emission spectra of individual NCs.[15] Finally, a recent report attributed the suppression of Auger recombination in CdZnSe/ZnSe NCs to the formation of a "smooth" confining potential resulting from a graded composition of the NC interfacial layer.[16] This explanation is based on recent theoretical work, which directly links the Auger decay rate to the steepness of the interfacial potential.[17]

In our present study, we analyze dynamical and spectral properties of multiexcitons in a novel class of NCs that comprise a CdSe core and a thick CdS shell of up to 19 CdS monolayers (Figure 1a,b); see also Figure S1 in the Supporting Information. We developed these so-called "giant" NCs (g-NCs) in an attempt to improve chemical- and photostability against ionization by isolating a small emitting core from its chemical environment with a thick shell (single-composition or graded composition) of a wider-gap material and to effectively create a solution-phase structural mimic of an epitaxial quantum dot.[18] It was also hypothesized that this approach would lead to suppressed PL blinking, as the thick shell would prevent carriers from leaving the NC, inhibiting the formation of non-emitting charged NCs.[7,8] The synthesized g-NCs indeed exhibited greatly improved chemical- and photostability and suppressed blinking,[18] a result that has been confirmed by an independent study of similar structures.[19] Recently it has been shown that individual CdSe/CdS g-NCs can still emit even when they are charged (so-called "gray" states), and therefore, it is likely that previously observed reduced blinking is not only due to suppressed ionization but is also a consequence of extended Auger recombination lifetimes.[20] Here we demonstrate via direct dynamical studies of g-NC ensembles that Auger recombination is, indeed, very effectively suppressed in these nano-structures (by a factor of at least 75 relative to isoenergetic CdSe core-only NCs). As a result, even multiexcitons of a very high order (13th and possibly higher) exhibit high emission efficiencies and contribute to optical gain. This allows us to obtain optical amplification over an unprecedented bandwidth of more than 500 meV and with record low excitation thresholds.

In the present work, we use g-NC samples consisting of CdSe seed particles emitting at ~2.2 eV (Figure 1c). The emission energy shifts to the red by more than 200 meV upon deposition of the thick CdS shell (Figure 1d). On the basis of the energy offsets at the CdSe/CdS interface (Figure 1e), this shift occurs mostly as a consequence of electron delocalization into the shell region, while the hole remains primarily confined to the core (Figure 1f). The PL red shift is accompanied by a significant increase (almost 100-fold) of the absorption cross-section at high spectral energies (>2.4 eV) because in g-NCs high-frequency absorption is dominated by the CdS shell, which accounts for ~98% of the nanostructure volume. Typical PL quantum yields for the g-NCs are 50 to 60%.

To study exciton population dynamics, we time-resolve the PL using time-correlated single-photon counting (time resolution is 50 ps). The samples are excited by 200 fs pulses at 3.1 eV. An average initial NC occupancy following photoexcitation, $\langle N_0 \rangle = \langle N(t = 0) \rangle$, can be estimated from $\langle N_0 \rangle = \sigma j_p$, where $\sigma$ is the NC absorption cross-section and $j_p$ is the per-pulse photon fluence. We start our measurements with a sample of standard CdSe NCs (3 nm radius) overcoated with a thin ZnS shell[21] (referred to here as "reference") that emit at approximately the same wavelength as the g-NCs under investigation.

The pump-intensity dependent PL dynamics of the reference sample show trends that are typically observed for NCs (Figure 2a). At low pump fluences ($\langle N_0 \rangle \ll 1$), we observe a relatively slow, 24 ns decay that is dominated by radiative recombination of single excitons. At higher fluences, the measured dynamics develop a fast, subnanosecond initial component that is due to Auger decay of multiexcitons.[3,11] Because of the very short multiexciton lifetimes

limited by the Auger process, the PL traces show almost indistinguishable decay for $t > 2$ ns when all of the NCs are occupied with no more than one exciton. By extracting the fast decay component from the PL trace measured using a pump intensity that is just above the onset for the generation of multiexcitons,[3] we derive the biexciton lifetime $\tau_2$ ~200 ps (inset of Figure 2a). This value is consistent with previously measured biexciton Auger recombination times ($\tau_{2A}$) in CdSe NCs,[3,11] indicating that in this case biexcitons are essentially nonemissive and decay primarily via a nonradiative Auger process.

The PL time transients measured for the g-NC sample (Figure 2b) exhibit very different multiexciton dynamics. As in the reference sample, the low-pump-intensity decay in g-NCs is dominated by single excitons with a lifetime of 42 ns. At higher excitation intensities, the recorded traces again develop a faster multiexcitonic component, but in this case it persists for much longer than in the isoenergetic reference NCs and has an appreciable amplitude even at $t = 30$ ns after excitation. On the basis of the measured dynamics, we derive a biexciton lifetime of 10 ns (inset of Figure 2b). This value is 50 times longer than in the isoenergetic reference sample and thus indicates very significant suppression of Auger recombination.

On the basis of existing models of radiative decay in NCs, the radiative lifetime of a biexciton ($\tau_{2r}$) is shorter than that of a single exciton ($\tau_{1r}$) by a factor of 2 (for independent excitons) to 4 (for bulk-like recombination).[22] From PL relaxation dynamics and the quantum yield measured for the g-NCs at low pump fluences, $\tau_{1r}$ is from 42 to 57 ns (see Supporting Information, Figure S3), and hence, $\tau_{2r}$ ranges from 10.5 to 28.5 ns. We can further estimate a biexciton Auger lifetime in the g-NCs using the expression: $\tau_2^{-1}=\tau_{2r}^{-1}+\tau_{2A}^{-1}$ (here we neglect nonradiative decay channels other than Auger recombination). For $\tau_{2r} = 28.5$ ns, we obtain $\tau_{2A} = 15$ ns, which is 75 times longer than in a reference sample, indicating a significant reduction of Auger decay rates. Estimations using $\tau_{2r} = 10.5$ ns, yield $\tau_{2A} = 210$ ns, which points toward even greater, thousand-fold suppression of Auger decay. On the basis of the above calculations, we estimate that the intrinsic PL quantum yield of biexcitons in the g-NCs is from 34 to 95%. These tens of percent values are in sharp contrast to very low biexciton emission efficiencies in traditional NCs. For example, similar estimations conducted for a reference sample indicate the biexciton PL yield from ~1.8 to 3.4%.

We would like to point out that the above estimations are based on ensemble results, and hence represent an average over well-passivated, highly emissive g-NCs and poorly emitting particles that are still affected by trapping at interfacial defects. Our recent studies of individual “bright” g-NCs are consistent with nearly complete suppression of Auger decay as indicated, for example, by a linear scaling of spectrally integrated PL signal observed across orders of magnitude changes in pump intensity which extends well above the onset for multiexciton generation.

Very long multiexciton lifetimes are also evident from pump-intensity dependent studies of PL (Figure 2c,d). In the reference CdSe/ZnS NCs, pump-intensity dependences of PL signals measured at different times after excitation are indistinguishable at $t \gg \tau_{2A}$. In this case, all of the multiexcitons have decayed via the Auger process and the emission intensity is simply determined by the total number of photoexcited NCs independent of their early time occupancies. This behavior is evident from the data in Figure 2c, where the pump-intensity dependences recorded at $t \geq 2$ ns converge to a single saturation curve independent of the exact delay time used in the PL measurements. As expected, the measured long-lived PL signals closely follow the pump-intensity-dependent evolution of the total number of photoexcited NCs calculated assuming Poisson statistics of photon absorption events (red solid line in Figure 2c): $I_{PL}(t \gg \tau_2) \propto (1 - p_0) = (1 - \exp(-\langle N_0 \rangle))$, where $p_0$ is the fraction of un-excited NCs.[2]

The situation is clearly different for g-NCs (Figure 2d). Specifically, in this case, the PL pump-intensity dependence evolves on a much longer time scale and "stabilizes" only at $t > 50$ ns. This slow evolution is a result of the slow decay of multiexcitons. Because of their contribution to emission, the PL pump-intensity dependences measured at $t < 50$ ns significantly deviate from the $(1 - p_0)$ Poisson term (red solid line in Figure 2d). Only at very long times ($t > 60$ ns) does the PL intensity exhibit the $(1 - p_0)$ dependence, indicating that all of the multiexcitons have finally decayed and only single excitons are present in the system.

There are several factors that can potentially lead to suppression of Auger recombination in g-NCs: changes in the effective extent of electronic wave functions, altered electron–hole overlap and exciton–exciton repulsion, and/or the influence of interfaces. We consider each here. Typically, Auger lifetimes exhibit linear scaling with NC volume ("V-scaling"; see Supporting Information, Figure S4).[3,11] Therefore, the large spatial extent of the electronic wave functions in g-NCs is expected to lead to increased biexciton lifetimes. However, based on simple V-scaling, we obtain that the Auger lifetime in g-NCs can be longer than that in the reference sample by only a factor of up to ca. 6, which yields $\tau_{2A}$ of ~1.2 ns. This value is more than an order of magnitude smaller compared to an estimated lower limit of Auger lifetime in g-NCs (15 ns), indicating that the V-scaling arguments alone cannot explain significant slowing of multiexciton dynamics in g-NCs.

Second, as was mentioned earlier, g-NCs exhibit partial spatial separation between electrons and holes (holes are confined to the g-NC core while electrons are delocalized over its entire volume). This situation results in a reduced electron–hole overlap integral ($\theta_{eh}$) that could decrease the rate of Auger decay.[13,23] In our case, the calculated value of $\theta_{eh}$ is ~0.6 (inset of Figure 1f), which agrees well with the observed increase in single-exciton lifetime upon deposition of a shell. Taken together with V-scaling, the reduction of $\theta_{eh}$ can extend the Auger lifetime to ~2 ns, which is still not sufficiently long to explain experimental observations.

Third, we consider exciton–exciton repulsion.[24,25] As mentioned previously, this effect is possible in heterostructures that are characterized by either complete (type-II) or partial (quasi-type-II) spatial separation between electron and hole wave functions.[24] In such nanostructures, repulsive Coulomb interactions provide an additional driving force that together with an energy gradient at a heterointerface, helps to keep electrons and holes apart, thereby reducing the rate of Auger recombination. Our calculations predict that the partial spatial separation between electrons and holes occurringing-NCs can indeed produce appreciable exciton–exciton repulsion (see Supporting Information, Figure S2b). This effect is evident from the measured time-resolved PL spectra that indicate a transient red shift of the PL maximum (inset of Figure 2d). The fact that multiexciton recombination is accompanied by a decrease in the emission energy implies that the average per-exciton energy in a multiexciton is higher than that of a single exciton. Such an observation is a signature of exciton–exciton repulsion.[13,25] While the above measurements clearly show the existence of exciton–exciton repulsion in g-NCs, they also indicate that the repulsion energy is quite low, ~10 meV (see Supporting Information, Figure S2b). Since this value is smaller than thermal carrier energies at room temperature, it is unlikely to produce any appreciable effect on Auger decay. For example, even in type-II CdS/ZnSe NCs with a Coulomb repulsion energy on the order of 100 meV[13,25] (i.e., much greater than the room temperature thermal energy), Auger recombination still occurs on a subnanoseconds time scale.[13]

Finally, we analyze the effect of NC interfaces on Auger decay rates. According to Efros,[17] Auger recombination in NCs primarily takes place at interfacial regions and the likelihood of this process is highly sensitive to the steepness of the interface potential.[16] The difference in interfacial properties may, for example, explain a dramatic distinction in multiexciton dynamics in colloidal and epitaxial quantum dots. It is well established that Auger

recombination is not efficient in quantum dots fabricated by physical methods such as molecular beam epitaxy,[26] while it is extremely fast and efficient in colloidal NCs.[3] Epitaxial dots are typically embedded in a matrix of a wide-gap semiconductor such as ZnSe at temperatures high enough to produce interfacial alloying.[27,28] The "smoothness" of the resulting interfacial potential can be responsible for suppression of Auger recombination in these structures. This situation is in contrast to typical colloidal NCs that are characterized by sharp interfaces (semiconductor/solvent or semiconductor/ligands) with very large energy gradients. The interfacial properties of g-NCs are likely similar to those of epitaxial dots. Despite a moderate growth temperature (240 °C), the long reaction time (it takes ~40 h to fabricate a sample with a 10 monolayer CdS shell) can lead to significant interdiffusion of anions between the core and the shell, which could result in the formation of an intermediate alloyed layer with a smoothed potential. The formation of a graded interfacial layer has recently been invoked to explain the reduced efficiency of Auger decay in core–shell CdZnSe/ZnSe NCs.[16]

To summarize the above discussion, while factors such as a large volume, partial charge separation, and exciton–exciton repulsion each by itself may not be sufficient to explain the observed reduction of Auger rates in g-NCs, they may still impart an important effect on the Auger process when taken in aggregate. On the other hand, previous studies of epitaxial quantum dots[27,28] as well as recent models proposed for Auger recombination in NCs[17,29] emphasize the role of interfacial effects. Therefore, a reduced steepness of interfacial potential in g-NCs may play an especially important role in suppression of Auger decay in these nanostructures.

The suppression of Auger recombination can greatly benefit NC lasing applications. If exciton–exciton coupling is neglected, optical gain in NCs necessarily involves stimulated emission from multiexciton states.[4,13] In this case, optical gain dynamics are usually controlled by Auger recombination, which limits the optical-gain lifetime to tens of picoseconds. Auger recombination also imposes severe constraints on the spectral bandwidth of optical amplification. Optical gain due to biexcitons has a spectral width that is typically just a small fraction of the total width of the band-edge spontaneous PL.[4] The extension of optical gain to higher energies is only possible through stimulated emission by higher-order multiexcitons. Such multiexcitons, however, have lifetimes that are even shorter than those of biexciton states. This is because of the rapid scaling of Auger rate with the number of multiexcitons ($N$). For instance, in CdSe NCs it changes from quadratic to cubic with increasing NC size.[11] As a result, optical gain due to higher-order multi-excitons is extremely short-lived and typically not usable for optical amplification. Therefore, most reports on optical amplification in NCs only show amplified spontaneous emission (ASE) due to the lowest-energy band-edge transition, and very few studies[30,31] have demonstrated ASE due to transitions that also involve the second (1P) electron quantization shell. Optical gain due to states above the 1P level has never been observed in standard NCs because of a dramatic reduction of multiexciton emission yields for large NC occupancies ($N > 13$) that are required to "invert" the population of the third (1D) quantization shell (multiexciton Auger lifetimes scale faster with $N$ than their radiative times). Further, carrier lifetimes expected for such occupancies become comparable to thermalization times,[4] greatly complicating the establishment of the regime of population inversion.

On the basis of the observations of long multiexciton lifetimes in g-NCs and a corresponding increase in multi-exciton emission yields, one may expect that these samples could allow for extension of optical amplification bandwidth through the involvement of higher-order multiexcitons. Such spectral extension is indeed observed experimentally. The results of our ASE studies for g-NCs with an 11-monolayer shell in a close-packed film are summarized in Figure 3. At low excitation fluences, we observe spontaneous band-edge emission at 1.95 eV. At a fluence of 30 $\mu$J cm$^{-2}$, a narrower peak develops on the higher energy side (1.99 eV) of

the spontaneous emission band (Figure 3a), that together with a superlinear dependence on pump fluence (Figure 3b) indicates the ASE process. The blue shift of this ASE feature with regard to the spontaneous emission band is consistent with a repulsive character of exciton–exciton interactions in the g-NCs as discussed above.

As the pump fluence increases further, we detect two higher-energy ASE peaks (at 2.19 and 2.34 eV) that are likely due to optical transitions involving the second and the third quantization shells, respectively. Within a simple particle-in-a-box model,[32] the third electron quantized level becomes occupied only if the NC contains at least 9 excitons while the regime of population inversion only establishes for $N > 13$. The latter value is consistent with the pump fluence that is required to excite the third ASE feature, which corresponds to $\langle N_0 \rangle \sim 11$. These observations imply that multiexcitons of the 13th order (and possibly even higher) are sufficiently long-lived and sufficiently "bright" in g-NCs to produce the ASE effect. In standard CdSe NCs with a similar energy gap, the respective Auger lifetime would be less than 1 ps, shorter than typical optical gain build-up times, and hence not long enough for the establishment of the ASE regime.

As a result of the participation of higher-order multiexcitons, the optical gain of g-NCs in a dilute solution measured using transient absorption exhibits an unprecedented bandwidth of ~500 meV (Figure 3c). This large bandwidth is highly unusual not only for NC samples (open circles in Figure 3c) but also for other typical gain media such as laser dyes (dye gain bandwidths are typically <300 meV). These results imply that using a single g-NC sample one can tune the lasing color almost over the entire range of visible wavelengths by simply adjusting a laser cavity (see also Supporting Information, Figure S5). Furthermore, such bandwidth is sufficiently large to support femtosecond laser pulses.

The g-NC samples also show remarkably low ASE thresholds that result from increased absorption cross sections in addition to suppressed Auger decay. Specifically, in a reference NC sample, the excitation threshold for the band edge biexcitonic ASE is ~300 $\mu$J cm$^{-2}$, while it is only ~26 $\mu$J cm$^{-2}$ in g-NCs (squares in Figure 3b). Interestingly, excitation thresholds for the second (~100 $\mu$J cm$^{-2}$) and the third (~220 $\mu$J cm$^{-2}$) ASE features, which are due to higher-order multiexcitons, are still lower than that for biexcitonic gain in the reference sample.

In conclusion, we show that g-NCs consisting of a small CdSe core overcoated with a thick CdS shell show very long multiexciton lifetimes (~10 ns for a biexciton state) that indicate a significant, possibly complete, suppression of Auger recombination in these nanostructures. We discuss possible reasons for this suppression including the large effective volume of these NCs and a peculiar spatial distribution of electronic wave functions, which results in reduced electron–hole overlap and weak exciton–exciton repulsion. We conclude that while the above factors could indeed provide some reduction of Auger recombination rates, there may also be an important contribution from smoothing of the interfacial potential that results from the likely formation of a gradient alloy layer at the core/shell interface. This would be analogous to the situation in epitaxial quantum dots, where Auger recombination is an inefficient process. As a final proof of suppression of Auger recombination, we conduct ASE experiments. The ASE measurements indicate an extraordinarily large bandwidth of optical gain (>500 meV) that results from contributions of multiexcitons of high order to stimulated emission.

## Supplementary Material

Refer to Web version on PubMed Central for supplementary material.

## Acknowledgments

This work was supported by the Chemical Sciences, Biosciences, and Geosciences Division of the Office of Basic Energy Sciences, U.S. Department of Energy (DOE) and Los Alamos LDRD funds. V.I.K. and J.A.H acknowledge partial support from the Center for Integrated Nanotechnologies jointly operated for DOE by Los Alamos and Sandia National Laboratories. J.A.H. also acknowledges partial support from NIH NIGMS Grant 1R01GM084702-01. F.G.-S. and J.V. are Los Alamos National Laboratory Director's Fellows.

## References

1. Alivisatos AP. Science 1996;271:933–937.
2. Klimov, VI. Semiconductor and metal nanocrystals. Marcel Dekker; New York: 2003.
3. Klimov VI, Mikhailovsky AA, McBranch DW, Leatherdale CA, Bawendi MG. Science 2000;287:1011–1013. [PubMed: 10669406]
4. Klimov VI, Mikhailovsky AA, Xu S, Malko A, Hollingsworth JA, Leatherdale CA, Eisler HJ, Bawendi MG. Science 2000;290:314–317. [PubMed: 11030645]
5. Nozik AJ. Physica E 2002;14:115–120.
6. Anikeeva PO, Madigan CF, Halpert JE, Bawendi MG, Bulovic V. Phys Rev B 2008;78:085434.
7. Nirmal M, Dabbousi BO, Bawendi MG, Macklin JJ, Trautman JK, Harris TD, Brus LE. Nature 1996;383:802–804.
8. Efros AL, Rosen M. Phys Rev Lett 1997;78:1110–1113.
9. Chepic DI, Efros AL, Ekimov AI, Vanov MG, Kharchenko VA, Kudriavtsev IA, Yazeva TV. J Lumin 1990;47:113–127.
10. Wang LW, Califano M, Zunger A, Franceschetti A. Phys Rev Lett 2003;91:056404. [PubMed: 12906614]
11. Klimov VI, McGuire JA, Schaller RD, Rupasov VI. Phys Rev B 2008;77:195324.
12. Htoon H, Hollingsworth JA, Dickerson R, Klimov VI. Phys Rev Lett 2003;91:227401. [PubMed: 14683270]
13. Nanda J, Ivanov SA, Achermann M, Bezel I, Piryatinski A, Klimov VI. J Phys Chem C 2007;111:15382–15390.
14. Nanda J, Ivanov SA, Htoon H, Bezel I, Piryatinski A, Tretiak S, Klimov VI. J Appl Phys 2006;99:034309.
15. Osovsky R, Cheskis D, Kloper V, Sashchiuk A, Kroner M, Lifshitz E. Phys Rev Lett 2009;102:197401. [PubMed: 19518993]
16. Wang X, Ren X, Kahen K, Hahn MA, Rajeswaran M, Maccagnano-Zacher S, Silcox J, Cragg GE, Efros AL, Krauss TD. Nature 2009;459:686–689. [PubMed: 19430463]
17. Efros, AL. Auger processes in nanosize semiconductor crystals. In: Efros, AL.; Lockwood, DJ.; Tybeskov, L., editors. Semiconductor nanocrystals. Kluwer academic/Plenum Publishers; New York: 2003. p. 52-71.
18. Chen Y, Vela J, Htoon H, Casson JL, Werder DJ, Bussian DA, Klimov VI, Hollingsworth JA. J Am Chem Soc 2008;130:5026–5027. [PubMed: 18355011]
19. Mahler B, Spinicelli P, Buil S, Quelin X, Hermier JP, Dubertret B. Nat Mater 2008;7:659–664. [PubMed: 18568030]
20. Spinicelli P, Buil S, Quelin X, Mahler B, Dubertret B, Hermier JP. Phys Rev Lett 2009;102:136801. [PubMed: 19392384]
21. Hines MA, Guyot-Sionnest P. J Phys Chem 1996;100:468–471.
22. McGuire JA, Joo J, Pietryga JM, Schaller RD, Klimov VI. Acc Chem Res 2008;41:1810–1819. [PubMed: 19006342]
23. Oron D, Kazes M, Banin U. Phys Rev B 2007;75:035330.
24. Piryatinski A, Ivanov SA, Tretiak S, Klimov VI. Nano Lett 2007;7:108–115. [PubMed: 17212448]
25. Klimov VI, Ivanov SA, Nanda J, Achermann M, Bezel I, McGuire JA, Piryatinski A. Nature 2007;447:441–446. [PubMed: 17522678]

26. Dekel E, Gershoni D, Ehrenfreund E, Spektor D, Garcia JM, Petroff PM. Phys Rev Lett 1998;80:4991–4994.
27. Kegel I, Metzger TH, Lorke A, Peisl J, Stangl J, Bauer G, Garcia JM, Petroff PM. Phys Rev Lett 2000;85:1694–1697. [PubMed: 10970591]
28. Liu N, Tersoff J, Baklenov O, Holmes AL, Shih CK. Phys Rev Lett 2000;84:334–337. [PubMed: 11015904]
29. Pandey A, Guyot-Sionnest P. J Chem Phys 2007;127:104710. [PubMed: 17867772]
30. Htoon H, Hollingworth JA, Malko AV, Dickerson R, Klimov VI. Appl Phys Lett 2003;82:4776–4778.
31. Chan Y, Caruge JM, Snee PT, Bawendi MG. Appl Phys Lett 2004;85:2460–2462.
32. Efros AL, Efros AL. Sov Phys Semicond 1982;16:772–775.

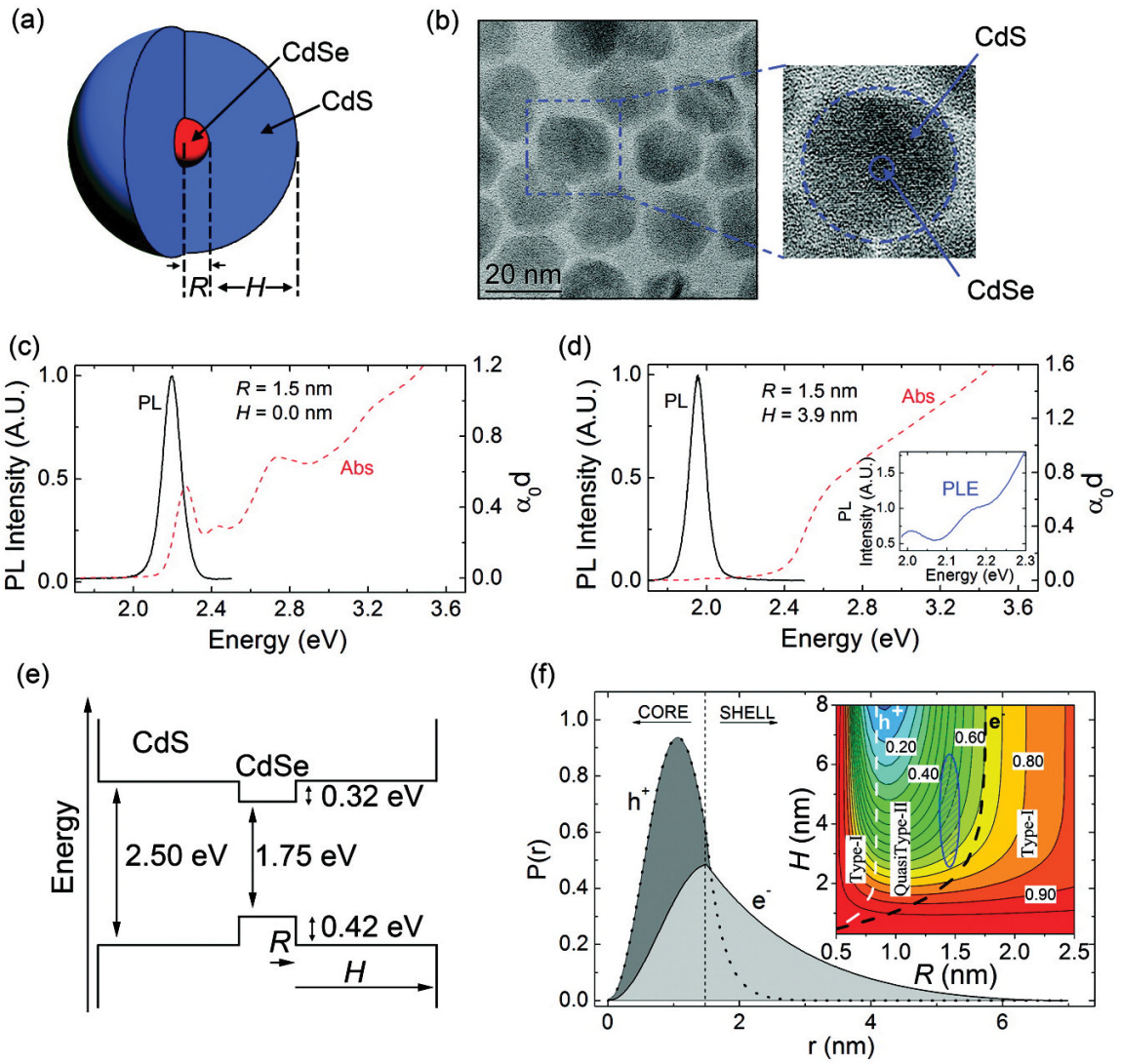


**Figure 1.**

(a) A schematic of the g-NC structure where *R* is the CdSe core radius and *H* is the CdS shell thickness. (b) A transmission electron microscopy image of g-NCs with *R* = 1.5 nm and *H* = 6.7 nm. Blue lines in the expanded view on the right illustrate the relative size of a core compared to the total size of a g-NC. (c) PL (solid black line) and absorption (dashed red line) spectra for CdSe core-only NCs. (d) Upon growing a 3.9 nm thick shell of CdS on the 1.5 nm radius CdSe cores, the PL red shifts by ~200 meV and the absorption becomes dominated by the CdS shell. Inset: the PL excitation spectrum (monitored at 1.95 eV), which shows the structure of band-edge transitions due to the CdSe core. (e) Band alignment diagram of bulk CdSe and CdS. (f) Spatial probability distribution of the hole (dark gray area) and electron (light gray area) for *R* = 1.5 nm and *H* = 5.0 nm. The inset shows a contour plot of the calculated electron–hole overlap integral. White and black lines are boundaries between regions of (*R*,*H*)-space that correspond to different localization regimes. These lines are calculated from the condition that the probabilities of finding an electron (white dashed line) or a hole (black dashed line) in the core and the shell are equal to each other. The shaded elliptical area shows an approximate range of parameters of g-NCs studied in this work.

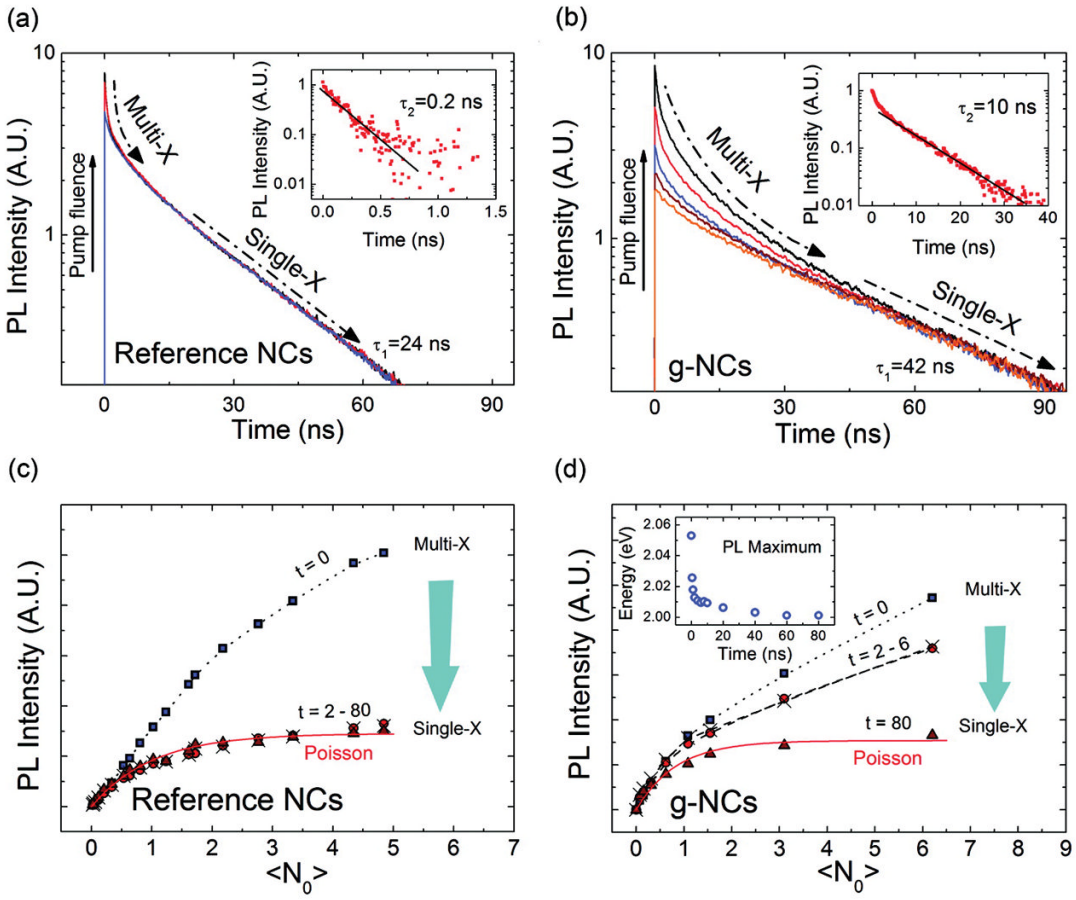


**Figure 2.**

(a) Time-resolved PL intensity of reference CdSe/ZnS core–shell NCs (dilute hexane solution) emitting at 1.92 eV for different excitation fluences (2 to 200 $\mu J/cm^2$); pump photon energy is 3.1 eV. Traces normalized at $t$ = 60 ns completely overlap at $t$ > 2 ns, indicating that relatively early in time all of the multiexcitons have already decayed. $\tau_1$ is the single exciton lifetime. Inset: the extracted biexciton dynamics show the 200 ps decay due to Auger recombination. (b) The same for g-NCs (12 monolayer CdS shell, $R$ = 1.5 nm and $H$ = 3.9 nm); PL is monitored at 2.00 eV. Traces normalized at $t$ = 90 ns become indistinguishable only for $t$ > 40 ns, indicating that in this case multiexcitons are long-lived. Inset: The extracted biexciton dynamics shows slow 10 ns decay. (c) PL intensity for reference CdSe/ZnS NCs as a function of NC average occupancy, $<N_0>$, measured at different times after excitation (symbols). Because of rapid Auger recombination of multiexcitons, the PL intensity saturates according to $(1 - p_0)$ (shown by the red line) for times longer than the biexciton lifetime. As a result, the dependences measured at $t$ = 2 and 80 ns are almost identical. (d) The same for g-NCs. Here, the PL intensity also exhibits saturation but at much longer times ($t$ > 60 ns) owing to the dramatically increased lifetime of multiexcitons. The inset shows a transient red shift of the emission maximum as a function of time for $<N_0>$ = 0.7. This red shift is a signature of exciton–exciton repulsion.

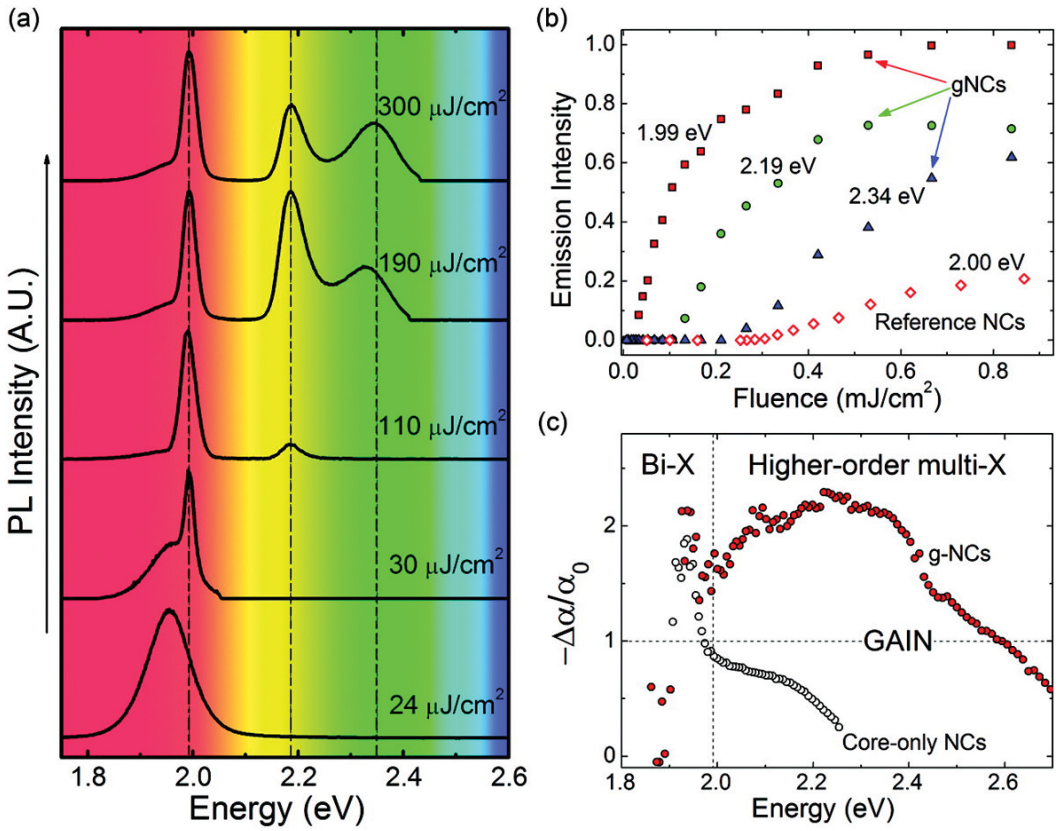


**Figure 3.**

(a) Emission spectra of a close-packed film of g-NCs (11 monolayer CdS shell) measured using 3.1 eV, 100 fs pump pulses with different per-pulse fluences (indicated in the figure); the pump-spot diameter is 60 $\mu$m. These spectra illustrate the development of three ASE peaks at 1.99, 2.19, and 2.34 eV that span the range of colors from red to green. (b) Emission intensity versus pump fluence at the positions of three ASE peaks observed for g-NCs (solid symbols) in comparison to the pump-fluence-dependent PL intensity for reference CdSe/ZnS NCs (hollow diamonds). (c) A normalized transient absorption spectrum of g-NCs (dilute hexane solution) shortly after excitation ($t$ = 2 ps) with 3.1 eV, 1.2 mJ cm$^{-2}$ pulses (red solid circles); this spectrum is calculated as a ratio of the measured pump-induced absorption bleaching ($\Delta\alpha < 0$) and ground-state absorption ($\alpha_0$). In this representation, optical gain corresponds to the situation where $-\Delta\alpha/\alpha_0 > 1$. Black open circles show the gain spectrum for core-only CdSe NCs recorded using an excitation fluence which corresponds to maximum gain bandwidth.